CHEMICAL ENGINEERING TRANSACTIONS
VOL. 88, 2021
A publication of AIDIC
The Italian Association of Chemical Engineering
Online at www.cetjournal.it
Guest Editors: Petar S. Varbanov, Yee Van Fan, Jiří J. Klemeš

ISBN 978-88-95608-86-0; **ISSN** 2283-9216
DOI: 10.3303/CET2188208

Multi-physics Coupling Simulation of Heat Transfer and Structural Optimization for a Three-phase Gas Insulated Switchgear Busbar

Bo Wang[a], Wenrong Si[c], Chenzhao Fu[c], Xiaoyu Jia[b], Zunrong Tang[a], Jian Yang[a,*], Qiuwang Wang[a]

[a] MOE Key Laboratory of Thermo-Fluid Science and Engineering, Xi'an Jiaotong University, Xi'an 710049, China
[b] Department of Fluid Machinery, School of Energy and Power Engineering, Xi'an Jiaotong University, Xi'an 710049, China
[c] State Grid Shanghai Electrical Power Research Institute, Shanghai 200437, China
yangjian81@mail.xjtu.edu.cn

Gas insulated switchgear (GIS) is one of the most important equipment in the power system. Excessive temperature of the GIS busbar conductor will lead to the loss of insulating gas performance and equipment life. In the present paper, based on the finite element method, the temperature distribution and power loss density of a 252 kV three-phase GIS busbar is numerically studied using electromagnetic-heat-flow coupling model, and the structure parameters of the rotation angle, center distance and conductor thickness of the busbar are optimized with Taguchi method. The results show that the conductor thickness has the greatest influence on the maximum temperature and power loss, and the influence proportion is more than 70 %. When the combination scheme of (A1, B5, C5) is adopted, the temperature rises and power loss performance of GIS has been optimized. The maximum temperature is reduced by 9.56 K and the power loss is reduced by 21.7 %. In addition, according to the analysis of the gas breakdown margin, it is found that the SF6 gas still has a good insulation performance after structure optimization. This study is of great significance to the heat transfer and optimization design of three-phase GIS busbar.

1. Introduction

Gas insulated switchgear (GIS) is an important power equipment in the field of power transmission and transformation engineering, its safety performance is related to the risk evaluation standard of International Electro Technical Commission (IEC) (Leva et al., 2012). Accurately calculating and reducing the operating temperature of the GIS busbar can improve the safety of the GIS in operation (Wu et al., 2020). And lower busbar temperature means less power loss in GIS, which will reduce unnecessary energy waste.

Kim et al. (2005) earlier proposed a magnetic-thermal coupling finite element method to predict the temperature rise of the busbar, took loss obtained from the magnetic field analysis as the heat source to calculate the temperature of the busbar, and this method is proved reliable by experiment. Chen et al. (2016) established a multi-physics coupled GIS busbar model based on the finite element method, changed the conditions of load current, ambient temperature, solar radiation and wind speed to study the factors that affect the temperature distribution. Lei et al. (2016) studied the thermal characteristics of the GIS busbar based on the electromagnetic-flow-thermal coupling model, and analyzed the temperature rise of the busbar with different conductor and enclosure diameters. Rebzani et al. (2016) proposed a method of changing the shape of the busbar conductor and slotting on the conductor to enhance the heat transfer of the GIS, and finally the maximum temperature of the conductor was reduced by 4 K. Based on the SF6 gas breakdown criterion, Wu et al. (2017) proposed a new busbar design method to reduce the busbar conductor temperature within the minimum breakdown margin.

The research based on the finite element method to obtain the temperature rise and temperature distribution of the busbar under multi-physics coupling has been relatively mature, but the research on optimizing the temperature rise of the busbar on this basis is still relatively few. In this paper, a finite element model of 252

Paper Received: 25 May 2021; Revised: 20 August 2021; Accepted: 11 October 2021
Please cite this article as: Wang B., Si W., Fu C., Jia X., Tang Z., Yang J., Wang Q., 2021, Multi-physics Coupling Simulation of Heat Transfer and Structural Optimization for a Three-phase Gas Insulated Switchgear Busbar, Chemical Engineering Transactions, 88, 1249-1254 DOI:10.3303/CET2188208

kV three-phase common box GIS busbar is established. After considering the skin effect, proximity effect, eddy current induction and thermal radiation, the temperature, velocity and breakdown margin distribution of the busbar are calculated under the coupling of electromagnetic-heat-flow multi physical field. And the Taguchi method is used to optimize the rotation angle, center distance and conductor thickness of the busbar conductor to achieve lower temperature rise and less power loss. This work can provide reference for GIS heat transfer calculation with multi-physical field coupling and GIS busbar structure optimization design.

2. Physical model and calculation method

2.1 Physical model and geometric parameters

In this study, a 252 kV three-phase common box GIS busbar is selected as the research object (Jin et al., 2013). This busbar structure is mainly composed of GIS enclosure, three busbar conductors and SF6 insulating gas. In order to simplify the calculation, the busbar is simplified into a two-dimensional model. Its physical model and size are shown in Figure 1.

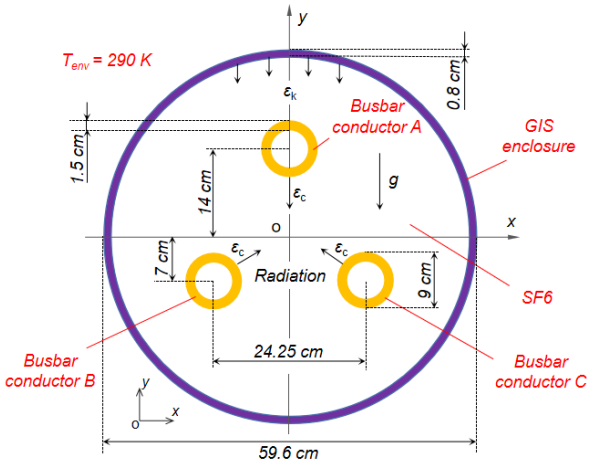

Figure 1: Physical model of 252 kV three-phase GIS busbar

Some physical properties of SF6 gas and busbar conductors change with temperature. SF6 gas physical properties are given by COMSOL finite element analysis software. The thermal conductivity and specific heat capacity of SF6 gas are show in Eq(1)-(2) (Wang et al., 2019). Where $c_{p,\ sf6}$ (T) is the constant pressure heat capacity of SF6 gas, J/(kg·K); λ_{sf6} (T) is the thermal conductivity of SF6 gas, W/(m·K); T is temperature, K. The ambient temperature T_{env} is 290 K, the Sutherland constant S of SF6 gas is 110.55 K.

$$c_{p,\ sf6}(T) = -2\times10^{-3}\times T^2 + 2.4\times T + 123.4 \tag{1}$$

$$\lambda_{sf6}(T) = 0.01206\times(T/T_{env})^{1.5}\times\left((T_{env}+S)/(T+S)\right) \tag{2}$$

σ (T) is the electrical conductivity of busbar conductors, S/m, as show in Eq(3).

$$\sigma(T) = 1/\rho_0\left(1+\alpha\left(T-T_{ref}\right)\right) \tag{3}$$

The electrical conductivity of conductors changes with temperature, the reference resistivity ρ_0 is 3.3 × 10^{-8} Ω·m, the resistivity temperature coefficient α is 4.0 × 10^{-3} 1/K, and the reference temperature T_{ref} is 293.15 K.

2.2 Control equations and calculation methods

The GIS model is divided into solid domain (conductors and enclosure) and fluid domain (SF6 gas). The electromagnetic-heat coupling equations of the solid domain are show in Eq(4)-(6). The heat transfer equation of conductors and enclosure Eq(4) and the electromagnetic filed equation Eq(6) are coupled by the magnetic loss equation Eq(5).

$$\nabla\cdot\left(\lambda(T)\nabla T\right) + Q_e = 0 \tag{4}$$

$$Q_e = Q_{rh} + Q_{ml} = \frac{1}{2}Re\left(\vec{J}\cdot\vec{E}^*\right) + \frac{1}{2}Re\left(j\omega\vec{B}\cdot\vec{H}^*\right) \tag{5}$$

$$-\omega^2\gamma\vec{A}+j\omega\sigma(T)\vec{A}+\nabla\times\left(\mu^{-1}\nabla\times\vec{A}\right)=0 \tag{6}$$

The constitutive equations of electromagnetic field are show in Eq(7)-(10).

$$\nabla\times\vec{A}=\vec{B} \tag{7}$$

$$\vec{E}=-j\omega\vec{A} \tag{8}$$

$$\vec{B}=\mu\vec{H} \tag{9}$$

$$\vec{J}=\sigma(T)\vec{E} \tag{10}$$

The coupled heat-flow equations of the fluid domain are show in Eq(11)-(13), the mass conservation equation Eq(11), the heat transfer equation Eq(12) and the momentum conservation equation Eq(13) are coupled by the thermal properties of SF6 gas (gas properties are given by COMSOL finite element analysis software).

$$\nabla\vec{v}=0 \tag{11}$$

$$\rho(T)(\vec{v}\cdot\nabla T)=\nabla\cdot[(\frac{\lambda(T)}{c_p(T)}+\frac{\mu_t}{\sigma_T})\cdot(\nabla T)] \tag{12}$$

$$\rho(T)(\vec{v}\cdot\nabla\vec{v})=-\nabla p+\nabla\cdot[(\mu(T)+\mu_t)(\nabla\vec{v}+(\nabla\vec{v})^T)]+\beta(T-T_0)\rho(T)g \tag{13}$$

Where λ (T) is the thermal conductivity, W/(m·K); Q_e is the total loss density of the busbar conductors and the enclosure, Q_{rh} and Q_{ml} are the electrical loss density and magnetic loss density, W/m^3; Re is the real part of the imaginary number; $\vec{J}$ is the current density, A/m^2; $\vec{E}^*$ and $\vec{H}^*$ are conjugate complex numbers of $\vec{E}$ and $\vec{H}$; $\vec{B}$ is the magnetic induction, T; $\vec{A}$ is the magnetic vector potential, Wb/m; $\vec{E}$ is the electric field strength, N/C; $\vec{H}$ is the magnetic field strength, A/m; j is an imaginary unit; ω = 2πf, is the phase angle; f is the electric excitation frequency, 50 Hz; γ is the dielectric constant, F/M; μ is the permeability, H/m; σ (T) is the electrical conductivity, S/m; $\vec{v}$ is the speed vector of SF6 gas, m/s; ρ (T) is the SF6 gas density, kg/m^3; c_p (T) is the constant pressure specific heat capacity of SF6 gas, J/(kg·K); μ_t is the turbulent viscosity of SF6 gas, kg/(m·s); σ_T is the Prandtl number of the SF6 gas heat transfer equation; p is pressure, Pa; μ (T) is the dynamic viscosity of SF6 gas, kg/(m·s); β is the volume expansion coefficient of SF6 gas; g is the gravitational acceleration, m/s^2; T_0 is the reference temperature, K.

The boundary condition of the contact surface between the SF6 gas and GIS enclosure and busbar conductors is fluid-solid coupling heat transfer boundary. The radiation heat transfer exists between the inner surface of GIS enclosure and the outer surface of busbar conductors, and the radiant emissivity, both ε_k and ε_c are 0.85. The heat transfer of the outer wall of GIS enclosure can be considered as natural convection heat transfer outside a horizontal cylindrical wall, and the ambient temperature, T_{env} is 290 K.

In the present study, the governing equations are solved with the finite element analysis software COMSOL Multiphysics 5.2, and the MUMPS solver is employed for the computations (COMSOL Multiphysics 5.2, 2016). The conservative interface flux conditions for mass, momentum, and heat transfer are adopted at the solid-fluid interfaces. When the calculated residual is less than 10^{-3}, the calculation is considered to have reached convergence.

3. Grid independence test and model validations

The memory resources required for multi-physics direct coupling method are extremely large, too fine meshing makes calculation impossible. In the current study, four sets of grids have been tested. The total number of four sets of grids are 6000, 7754, 10064 and 13132 respectively. Set the rated current to 3150 A, and use the maximal temperature at steady state as the basis for comparison. The results show that a grid-independent solution is obtained when the number of grids is 10064. To save computer computing resources, we adopted a grid division method with a grid number of 10064 for subsequent calculations.

In order to ensure the accuracy of simulation, it is necessary to verify the calculation model and method. The three-phase common box GIS heat transfer model of Novak and Koller (2012) is used for verification. The rated current is set as 3000 A and the alternating current frequency is 60 Hz. The model is calculated to the

steady state, and then the maximum temperature of each GIS component under the stable operation condition is compared with the experimental results (Novak and Koller, 2012). The simulation results of the maximum temperature of the bus conductors, GIS enclosure and SF6 gas are 336.05 K, 310.85 K and 328.25 K respectively, and the experimental results are 336.85 K, 307.35 K and 326.15 K respectively. The results show that the calculation model and method used in this study are reliable.

4. Results and discussion

In this article, numerical simulation and Taguchi method are used to optimize the structure parameters of a 252 kV three-phase GIS busbar with a rated current of 3150 A. The optimized parameters are respectively the angle (θ) of the three conductors rotating clockwise around the center of the GIS at the same time, the distance (d_0) between the center of the conductor and the center of the GIS, and the thickness (δ) of the conductors. For each optimized parameter, there are five different levels, as shown in Table 1. The targets that need to be reduced are the maximum temperature (T_{max}) and the power loss density (Q_h) of the GIS at steady-state operation.

Table 1: Optimized parameters and levels

Optimized parameters	Symbol	Levels				
		1	2	3	4	5
θ (°)	A	0	30	45	60	90
d_0 (mm)	B	80	100	120	140	160
δ (mm)	C	9	12	15	18	21

If all the parameters are combined separately for research, the calculation amount is relatively large. Therefore, the Taguchi method (Taguchi and konishi, 1987) is used to determine the numerical simulation calculation. There are a total of 25 cases that need to be simulated. Extract the maximum temperature (T_{max}) and power loss density (Q_h) in each case and convert them into the form of signal-to-noise ratio (SNR). Each optimized parameter (θ, d_0, δ) has a performance statistic value ($PS_{i,j}$), which represents the sum of the SNR of all cases with the optimized parameter i and the level j. The $PS_{i,j}$ of different optimized parameters at different levels are shown in Table 2. According to the calculation formula of SNR, $PS_{i,j}$ appears as a negative number, and the larger the $PS_{i,j}$, the lower the maximum temperature or power loss. The contribution rate (CR_i) represents the proportion of the influence of different optimized parameters on reducing the maximum temperature and power loss, and the calculation formula is show in Eq(14)-(15).

$$R_i = \max(PS_{i,j} \mid j = 1,2,3,4,5) / 5 - \min(PS_{i,j} \mid j = 1,2,3,4,5) / 5 \quad (i=A,B,C) \tag{14}$$

$$CR_i = R_i / \sum_i^3 R_i \quad (i=A,B,C) \tag{15}$$

Table 2: Performance statistics and contribution rates of different optimized parameters (I=3150 A)

Targets	Optimized parameters	$PS_{i,j}$					R_i	CR_i
		Level 1	Level 2	Level 3	Level 4	Level 5		
T_{max}	A (θ)	-253.53	-254.13	-253.65	-253.69	-253.68	0.12	8.3%
	B (d_0)	-254.83	-253.76	-253.47	-253.36	-253.26	0.31	21.5%
	C (δ)	-256.81	-254.82	-253.00	-252.25	-251.78	1.01	70.2%
Q_h	A (θ)	-291.48	-294.64	-292.07	-292.41	-292.33	0.63	6.5%
	B (d_0)	-299.83	-292.57	-290.63	-290.06	-289.84	2.00	20.7%
	C (δ)	-313.45	-300.88	-288.31	-282.02	-278.27	7.04	72.8%

According to Table 2, whether it is for the maximum temperature (T_{max}) or power loss density (Q_h), the conductor thickness (δ) has the largest contribution rate, which are 70.2 % and 72.8 %, respectively. Therefore, when optimizing the structure of three-phase GIS busbar, we can focus on the influence of conductor thickness. The center distance (d_0) also has a certain influence on reducing the maximum temperature and power loss, which are 21.5 % and 20.7 %, respectively. It can be optimized according to the actual situation. The change of the conductor rotation angle (θ) has the smallest effect on temperature and loss, both of which are below 10 %.

When the optimization target is the maximum temperature (T_{max}), level 1 of parameter A has the largest performance statistics (-253.53), which indicates that when the rotation angle (θ) is 0°, the maximum temperature is the lowest. In the same way, the level 5 of parameter B and the level 5 of parameter C both have the largest performance statistics. Therefore, using the combination scheme of (A1, B5, C5), the maximum temperature of the GIS busbar can be reduced to the greatest extent within the research range. Moreover, using the combination scheme of (A1, B5, C5), the power loss density can also be reduced to the minimum within the research range, according to table 2. So we adopt the combination scheme of (A1, B5, C5) to optimize the GIS busbar structure.

For the structure before optimization (θ=0°，d_0=140 mm，δ=15 mm), the average velocity (U_{ave}) of SF6 gas in the GIS is 0.018 m/s, the maximum temperature (T_{max}) of the busbar is 335.70 K, the minimum breakdown margin (E_{mmin}) (Wu et al., 2017) of SF6 gas calculated under 1050 kV lightning impulse withstand voltage (Cui et al., 2014) is 7.97 kV/mm, and the GIS power loss density (Q_h) is 729.5 W/m^3, as shown in Table 3. According to Figure 2, the following results can be obtained. (1) The flow field is symmetrically distributed in the vertical direction, and the maximum velocity appears on both sides of the wall due to the effect of gravity and the limitation of the enclosure. (2) The temperature field is also symmetrically distributed, and the temperature of the busbar conductor A is the highest. (3) Under the influence of electric field intensity and SF6 gas flow, the breakdown margin in the accessory regions of the three busbar conductors is the smallest.

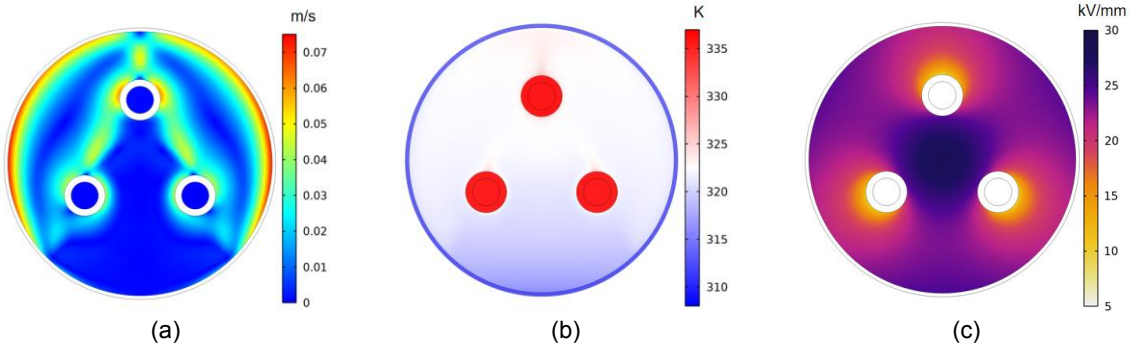

Figure 2: Simulation results of GIS before structure optimization (θ=0 °, d0=140 mm, δ=15 mm) of (a) velocity distribution, (b) temperature distribution and (c) breakdown margin distribution

The numerical calculation results of the GIS busbar after structure optimization (θ=0°，d_0=160 mm，δ=21 mm) are shown in Figure 3 and Table 3.

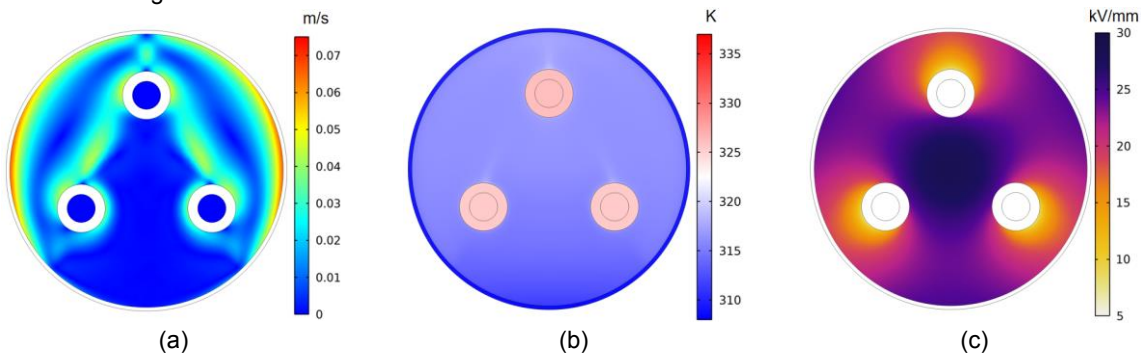

Figure 3: Simulation results of GIS after structure optimization (θ=0 °, d0=160 mm, δ=21 mm) of (a) velocity distribution, (b) temperature distribution and (c) breakdown margin distribution

Compare the results after optimization with the results before optimization, the following results can be obtained. (1) The distribution law of flow field, temperature field and breakdown margin has not changed. (2) The average velocity (U_{ave}) of SF6 gas changes 0.002 m/s, the maximum temperature (T_{max}) of GIS decreases by 9.56 K, and the power loss density (Q_h) decreases by 158.42 W/m^3, with a percentage decrease of 21.7 %. (3) The minimum breakdown margin (E_{mmin}) is reduced by 1.96 kV/mm, but it is still greater than 0 kV/mm (6.01 kV/mm), so SF6 gas still has good insulation performance.

Table 3: Comparison of u_{ave}, T_{max}, Q_h and E_{mmin} before and after structure optimization of GIS busbar

Conditions	U_{ave} ($m \cdot s^{-1}$)	T_{max} (K)	Q_h ($W \cdot m^{-3}$)	E_{mmin} ($kV \cdot mm^{-1}$)
θ=0 °, d_0=140 mm, δ=15 mm	0.018	335.70	729.50	7.97
θ=0 °, d_0=160 mm, δ=21 mm	0.016	326.14	571.08	6.01

5. Conclusions

The Taguchi method is used to optimize the structure of the three-phase GIS busbar, and the results after structure optimization are compared with those before optimization. The main findings are as follows:

(1) The change of conductor thickness has the greatest influence on the maximum temperature and power loss of the GIS, with a contribution rate of more than 70 %; the center distance has a certain influence on the temperature rise and loss, with a contribution rate of about 20 %; the influence of the rotation angle is the smallest, less than 10 % .

(2) When (A1, B5, C5) combination scheme is adopted, that is, the rotation angle is 0 °, the center distance is 160 mm, and the conductor thickness is 21 mm, the maximum temperature and power loss of GIS busbar all can reach a lower value.

(3) With the optimized GIS busbar structure, the maximum temperature is reduced by 9.56 K, the power loss density is reduced by 158.42 W/m^3, with a percentage decrease of 21.7 %, and the minimum breakdown margin of the GIS is reduced, but the SF6 gas still has good insulation performance.

This article has reference significance for the optimization design of the three-phase GIS busbar structure, but due to the simplification of the physical model, the results in this article may deviate from the actual situation. In the future, a three-dimensional GIS busbar model will be established to consider the influence of contact resistance on the maximum temperature and power loss.

Acknowledgment

This work was supported by the S &T project of State Grid Shanghai Municipal Electrical Power Company under grant number of 52094020005J.

References

Chen Q., Li Q.M., Cong H.X., Jin H., Peng Z.X., 2016, Numerical calculation and correlative factors analysis on temperature distribution of GIS bus bar based on coupled multi-physics methodology combined with multiple boundary conditions, Transactions of China Electrotechnical Society, 31, 187-195.

COMSOL Multiphysics® v. 5.2. cn.comsol.com, 2016, COMSOL AB, Stockholm, Sweden.

Cui H.J., Chen G.S., Liu T., 2014, Development of a new type small-sized 252 kV GIS, High Voltage Apparatus, 50, 105-108.

Huang M.D., Xiao C., Yang Z.N., Pang W.L., Wu X.X., 2020, Research progress of GIS equipment heating, High Voltage Apparatus, 56, 24-33.

Kim J.K., Hahn S.C., Park K.Y., Hong K.K., Oh Y.H., 2005, Temperature rise prediction of EHV GIS bus bar by coupled magnetothermal finite element method, IEEE Transactions on Magnetics, 41, 1636-1639.

Leva M.C., Pirani R., De Michela M., Clancy P., 2012, Human factors issues and the risk of high voltage equipment: Are standards sufficient to ensure safety by design?, Chemical Engineering Transactions, 26, 273-276.

Lei J., Zhong J.Y., Wu S.J., Wang Z., Guo Y.J., Qin X.Y., 2016, A 3-D steady-state analysis of thermal behavior in EHV GIS busbar, Journal of Electrical Engineering and Technology, 11, 781-789.

Novak B., Koller L., 2012, Steady-state heating of gas insulated busbars, Transmission and Distribution Conference and Exposition (T&D), Orlando, USA, 1-7.

Rebzani N., Clavel E., Marty P., Morin A., 2016, Numerical multiphysics modeling of temperature rises in gas insulated busbars, IEEE Transactions on Dielectrics and Electrical Insulation, 23, 2579-2586.

Taguchi G., Konishi S., 1987, Orthogonal arrays and linear graphs, American Supplier Institute, Dearborn, USA.

Wang Z.B., Liu S.P., Zhou H.Y., Rao Z.Q., Chen Y.L., Lu H., Ma G.M., 2019, Multiphysics simulation method for GIS epoxy spacer temperature, High Voltage Engineering, 45, 3820-3826.

Wu X.X., Cheng S.M., Zhou F., Wu S.P., Feng Y., 2020, Influence of temperature rise due to rated-current flowing through busbar on the internal insulation characteristics of GIS, High Voltage Apparatus, 56, 7-14.

Wu X.X., Zhang K.J., Yu G.Z., Fang L., Wu S.P., Zhang J.G., 2017, Optimal design of gas insulated substation bus bar based on breakdown criteria of SF6 gas, High Voltage Engineering, 43, 1950-1957.